NUMERICAL STUDY OF NATURAL CONVECTION IN A SQUARE CAVITY UNDER NON-BOUSSINESQ CONDITIONS

by

Saber HAMIMID [a*], Messaoud GUELLAL [a], and Madiha BOUAFIA [b]

[a] LGPC, University of Setif 1, Setif, Algeria
[b] LMEE, University of Evry, Val d'Essonne, France

Original scientific paper
DOI: 10.2298/TSCI130810084H

Natural convection in a differentially heated cavity has been carried out under large temperature gradient. The study has been performed by direct simulations using a two-dimensional finite volume numerical code solving the time-dependent Navier-Stokes equations under the low Mach number approximation. The low Mach number model constitutes an important numerical problem for low speed flows. It is based on the filtering of acoustic waves from the complete Navier-Stokes equations. Various simulations were conducted including constant or variable transport coefficients and both small and large temperature differences. A comparison between an incompressible code based on the Boussinesq approximation and the low Mach number compressible code shows that the incompressible model is not sufficient to simulate natural convective flow for large temperature differences.

Key words: *natural convection, low Mach number approximation, numerical simulation*

Introduction

Natural convection in differentially heated cavities has received considerable attention in the literature due to its potential to model numerous applications of engineering interest. The majority of the published investigations involve small temperature difference for which the Boussinesq approximation is used which assumes that fluid properties are constant except a linear density dependence on the temperature in the buoyancy term. The limits of validity of the Boussinesq approximation have been investigatesd in [1-5]. In many physical and industrial applications such as thermal insulation systems, chemical vapor deposition reactors, atmospheric flows and combustion process, the temperature differences reach tens and hundreds of degrees. In such situations all assumptions used to justify the Boussinesq approximation fail and a different modeling approach is required, one that accounts for realistic non-linear fluid property variations. In this study, the low Mach number (LMN) approximation suggested by Paolucci [1] is used to solve the momentum and energy equations which lead to take into account fluid flows under large temperature gradients and variable transport coefficients.

In the LMN model, the complete Navier-Stokes equations are expanded in powers of a small parameter M^2 (M is the Mach number) and the total pressure p is decomposed into two terms: a mean thermodynamic pressure which is spatially uniform and depends on time

* Corresponding author; e-mail: sab_hamimid@yahoo.fr

$\bar{p}(t)$ and a dynamic pressure p_{dyn} [1] $p(x, y, t) = \bar{p}(t) + p_{dyn}(x, y)$. Since for low speed flows the thermodynamic pressure is very high compared to the dynamic pressure, this later can be neglected, *i. e.*, the dependence of the density on the dynamic pressure component can be eliminated and hence, the acoustic effects can be filtered out.

The purpose of this study is to combine the effects of a large temperature gradient and temperature-dependent viscosity and conductivity on the flow and heat transfer. A comparison between solutions issued from incompressible and compressible models is performed for both small and large temperature difference boundary conditions.

Problem definition and governing equations

Consider a flow of air in a square 2-D cavity of side H filled with air. The cavity is differentially heated, left and right walls are isothermal at T_h and T_c respectively ($T_h > T_c$) and horizontal walls are adiabatic. A Cartesian (x, y) co-ordinate system is selected with y pointing vertical and x horizontal, thus, the gravitational vector $\vec{g}$ is downwards parallel to the y-co-ordinate. The air is initially at rest and at a uniform temperature $T_0 = (T_h > T_c)/2$ and pressure p_0. It is assumed to be an ideal gas with constant specific heats c_p and c_v of ratio $\gamma = 1.4$, and its dynamic viscosity and thermal conductivity are allowed to depend on temperature according to Sutherland laws. Using the mean temperature T_0 and the temperature difference $\Delta T = (T_h - T_c)$, we introduce the Boussinesq ratio $\varepsilon_b = \Delta T/2T_0$.

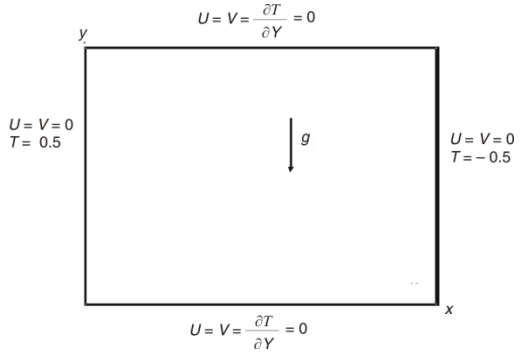

Figure 1. The flow configuration and co-ordinate system

Low Mach number model

We adopt the LMN approximation [6] to simulate a fluid flow submitted to large temperature differences. The governing equations are converted into the non-dimensional form by using the non-dimensional variables:

$$X = \frac{x}{H},\ Y = \frac{y}{H},\ U = \frac{uH}{\alpha_0},\ V = \frac{vH}{\alpha_0},\ \tau = \frac{t}{H^2/\alpha_0},$$

$$\Pi = \frac{pH^2}{\rho_0 \alpha_0^2},\ \overline{P} = \frac{\overline{p}}{p_0},\ \text{and}\ \ \theta = \frac{T - T_0}{T_h - T_c}$$

The thermo-physical properties (density, dynamic viscosity, thermal conductivity, thermal diffusivity) are scaled by ρ_0, μ_0, κ_0, and α_0 where the subscript 0 denotes values at the reference temperature T_0. The influence of the temperature on the specific heat is neglected which implies $c_p/c_{p0} = 1$.

$$\frac{\partial \rho^*}{\partial \tau} + \frac{\partial \rho^* U}{\partial X} + \frac{\partial \rho^* V}{\partial Y} = 0 \tag{1}$$

$$\rho^*\left(\frac{\partial U}{\partial \tau} + U\frac{\partial U}{\partial X} + V\frac{\partial U}{\partial Y}\right) = -\frac{\partial \Pi}{\partial X} + \mathrm{Pr}\left\{\frac{\partial}{\partial X}\left(\mu^*\frac{\partial U}{\partial X}\right) + \frac{\partial}{\partial Y}\left(\mu^*\frac{\partial U}{\partial Y}\right) + \frac{1}{3}\nabla\mu^*\nabla\vec{V}\right\} \tag{2}$$

$$\rho^*\left(\frac{\partial V}{\partial \tau}+U\frac{\partial V}{\partial X}+V\frac{\partial V}{\partial Y}\right)=-\frac{\partial \Pi}{\partial Y}-\mathrm{Ra}\,\mathrm{Pr}\frac{\rho^*-1}{2\varepsilon_b}+\mathrm{Pr}\left\{\frac{\partial}{\partial X}\left(\mu^*\frac{\partial V}{\partial X}\right)+\frac{\partial}{\partial Y}\left(\mu^*\frac{\partial V}{\partial Y}\right)+\frac{1}{3}\nabla\mu^*\nabla\vec{V}\right\} \quad (3)$$

$$\rho^* c_p^*\left(\frac{\partial \theta}{\partial \tau}+U\frac{\partial \theta}{\partial X}+V\frac{\partial \theta}{\partial Y}\right)=\frac{\partial}{\partial X}\left(k^*\frac{\partial \theta}{\partial X}\right)+\frac{\partial}{\partial Y}\left(k^*\frac{\partial \theta}{\partial Y}\right)+\frac{\gamma-1}{2\varepsilon_b\gamma}\frac{\mathrm{d}\overline{P}}{\mathrm{d}\tau} \quad (4)$$

$$\rho^*=\frac{\overline{P}}{2\varepsilon_b\theta+1} \quad (5)$$

where Π is the reduced pressure. An additional equation is given by calculating $\mathrm{d}\overline{P}/\mathrm{d}\tau$. Mass conservation eq. (1), combined with energy eq. (4) and state eq. (5) permit to write the divergence of velocity in the form given by eq. (6). By integrating this equation over the fluid domain, for $\mathrm{d}\overline{P}/\mathrm{d}\tau$ we obtain:

$$\nabla\vec{V}=\frac{-1}{\gamma\overline{P}}\frac{\mathrm{d}\overline{P}}{\mathrm{d}\tau}+\frac{2\varepsilon_b}{\overline{p}}\nabla k^*\nabla\theta \quad (6)$$

$$\frac{\mathrm{d}\overline{P}}{\mathrm{d}\tau}=2\varepsilon_b\gamma\frac{1}{\int_\Omega d\Omega}\int_S k^*\frac{\partial T}{\partial n}\mathrm{d}S \quad (7)$$

Furthermore, we need an equation to derive the thermodynamic pressure P. This equation is obtained from the conservation of mass:

$$\overline{P}=\frac{\int_\Omega \mathrm{d}\Omega}{\int_\Omega \frac{1}{2\varepsilon_b\theta+1}\mathrm{d}\Omega} \quad (8)$$

The governing equations are supplemented by Sutherland's law for the dynamic viscosity:

$$\mu^*(\theta)=(2\varepsilon_b\theta+1)^{3/2}\frac{1+S_\mu/T_0}{2\varepsilon_b\theta+1+S_\mu/T_0} \quad (9)$$

where S_μ =110.4 [7]. Using the Prandtl number, the conductivity is given by:

$$k^*(\theta)=\frac{\mu^*(\theta)}{\mathrm{Pr}} \quad (10)$$

In the Boussinesq limit ($\varepsilon_b \to 0$), substantial simplification of the above system can be implemented. Specifically, variation of the thermodynamic pressure and density can be ignored, and the velocity field can be treated as divergence free.

Numerical procedure

The numerical solution of the governing differential equations for the velocity, pressure and temperature fields is obtained by using a finite volume technique. A power scheme was also used in approximating advection-diffusion terms. The SIMPLER algorithm whose details can be found in Patankar [8], with a staggered grid is employed to solve the coupling between pressure and velocity. The governing equations are writing in transient form and a fully implicit transient differencing scheme was employed as an iterative procedure to reach steady state. The discretized equations are solved using the line by line Thomas algorithm with two directional sweeps.

Verification

The code employed in this paper has been verified by comparing our results with those in [9, 10]. Calculations were carried out for air initially at temperature T_0 = 600 K and for Ra = 10^6 and ε_b = 0.6. The test cases include workshops with constant and variable properties. Data presented in tab. 1, including average Nusselt numbers at the active walls and the pressure ratio p/p_0 show a good agreement with results of Heuveline [9] and Vierendeels [10].

Table 1. Air benchmark test cases [9, 10]

	[9]	[10]	Present work			
Test case 1 (Ra = 10^6, ε_b = 0.6 and constant properties)						
Nu(h)	8.859778	8.85978	8.85847			
Nu(c)	8.85978	8.85978	8.85847			
$\overline{p}/p_0$	0.85634	0.856340	0.85584			
Test case 2 (Ra = 10^6, ε_b = 0.6. and Sutherland law)						
Nu(h)	8.6889	8.6866	8.70078	8.69559	8.69355	8.68451
Nu(c)	8.6831	8.6866	8.70057	8.69166	8.69006	8.68316
$\overline{p}/p_0$	0.9249	0.924489	0.92498	0.92482	0.92495	0.92425
Type of mesh	400 000	2048 × 2048	300 × 300	360 × 360 (fine)	360 × 360 (very fine)	440 × 440 (very fine)

Results and discussions

The purpose of this section is to compare steady state solutions with an incompressible code (Boussinesq approximation) and a compressible code (LMN approximation). Both configurations are considered with the non-Boussinesq code: constant properties and temperature-dependent properties. Each test cases requires the specification of three dimensionless parameters (ε_b, μ, k), the other parameters such as the Prandtl number, the Rayleigh number and the aspect ratio are fixed to Pr = 0.71, Ra = 10^6 and A = 1. All the computations were performed with initial conditions: T_0 = 300 K, p_0 = 101325 Pa, and a stationary flow $\vec{V} = \vec{0}$.

Effect of the parameter ε_b

Table 2 summarizes the results in terms of Nu_{avg}, Nu_{max}, Nu_{min},$\bar{p}/p_0$ and ψ_{max} for different values of ε_b. Results indicate that there are opposite trends with ε_b concerning the maximum and minimum values of Nu on the two walls. On the hot side, Nu_{max} and Nu_{min} increase with increasing ε_b, while they decrease with increasing ε_b on the cold side. In addition, Nu_{max} is more important on the hot wall.

Table 2.Differentvalues of heat and flow parameters

	Constant properties					Sutherland law			
ε_b	BS	0.017	0.1	0.3	0.6	0.017	0.1	0.3	0.6
$Nu_{h,\ avg}$	8.823	8.825	8.825	8.832	8.854	8.824	8.819	8.784	8.656
$Nu_{c,\ avg}$	8.823	8.825	8.825	8.832	8.854	8.824	8.819	8.784	8.657
$Nu_{h,\ max}$	17.559	17.589	17.790	18.362	19.601	17.612	17.926	18.761	20.348
$Nu_{c,\ max}$	17.533	17.493	17.313	16.920	16.351	17.470	17.171	16.474	15.427
$Nu_{h,\ min}$	0.986	0.988	1.001	1.032	1.079	0.989	1.008	1.043	1.076
$Nu_{c,\ min}$	0.982	0.980	0.966	0.929	0.859	0.979	0.957	0.891	0.735
$\overline{p}/p_0$	–	0.999	0.996	0.967	0.856	0.999	0.998	0.984	0.935
ψ_{max}	16.825	16.834	16.854	16.936	17.153	16.836	16.860	16.867	16.721

The comparison is first done between steady state solutions obtained with the incompressible code and the compressible code with variable transport coefficients. The results focus on the following parameters: local Nusselt number, temperature θ and velocity components (U, V).

For low temperature differences (ε_b = 0.017), it is difficult to delineate between the Boussinesq and non-Boussinesq solutions. The predictions of incompressible and compressible models did not differ significantly and the solutions remain symmetric. These results are clearly seen in fig. 2 showing the local Nusselt number along the vertical walls, and in figs. 3-5 where horizontal profiles of temperature and vertical velocity are plotted at the mid-height (Y = 0.5) and horizontal velocity at the vertical section (X = 0.5) . It can be seen that the temperature and velocity profiles are very close to those of the boussinesq solution and are centro-symmetric with zero values at the cavity center. This symmetry is also found on the streamlines plotted for very weak compressible flows (fig. 6).

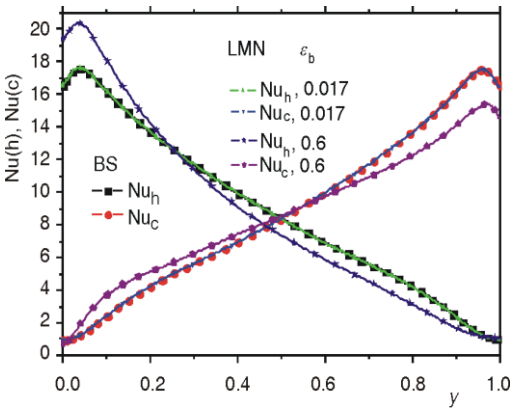

Figure 2. Local Nusselt number distributions on the vertical walls for different ε_b at Ra = 10^6 and variable properties

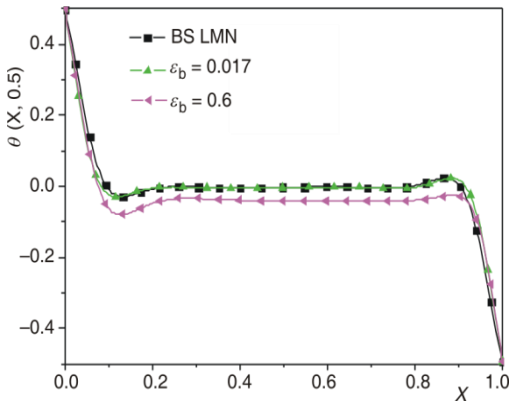

Figure 3. Cross-section of the temperature at mid-height cavity for Ra = 10^6 and Sutherland law

Under non-Boussinesq conditions and when the temperature difference increases (ε_b = 0.1, 0.3, 0.6), significant variation between incompressible and compressible solutions is observed. The symmetry seen in the previous case is broken due to the non-linear density and transport coefficients variations whose role is gradually strengthened as the flow becomes more compressible. The variations of local Nusselt numbers on the vertical walls are not symmetric (fig. 2). The maximum value is higher at the hot wall for the non-Boussinesq solution. The influence of the parameter ε_b on the temperature and velocities (U, V) is highlighted in figs. 3-5. By increasing ε_b non-Boussinesq profiles are distinguished from Boussinesq solutions. The influence is pronounced in the different boundary layers and at the core region where the temperature and horizontal velocity U vary significantly. In fig. 6, the streamlines show that the difference between the two solutions increases with the temperature difference and the centro-symmetry property disappears. In the Boussinesq formulation, the mass conservation is expressed as divergence-free and the solution is then symmetric. In the non-Boussinesq model, the mass conservation (eq. 1) and the non-zero divergence of velocity have a direct consequence on the flow symmetry. The asymmetry is due to the non-linear density which induces a dilatation of gas near the hot wall accelerating the upward flow and a contraction near the cold wall. As expected, this effect occurs in the boundary layers of the vertical velocity showing higher values near the hot wall (fig. 4) and consequently a greater heat flux through this wall (fig. 2).

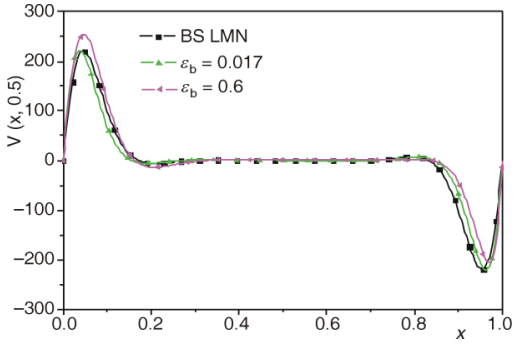

Figure 4. Vertical velocity at the horizontal cross-section at Y = 0.5 for Ra = 10^6 and variable properties

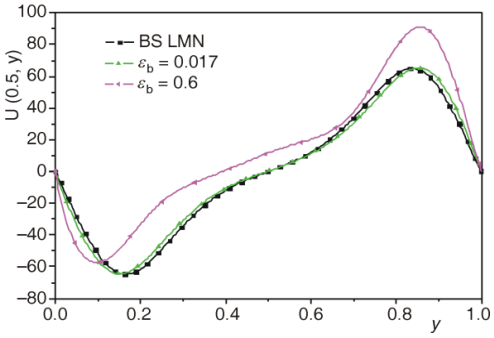

Figure 5. Horizontal velocity at the vertical cross-section at X = 0,5 for Ra = 10^6 and variable properties

A general aspect is observed on temperature and vertical velocity profiles. As the temperature difference increases, vertical boundary layers get thicker in the vicinity of the hot wall and thinner near the cold wall. From each profile, we can observe the two peaks moving slightly toward the cold wall. The peak value of the component velocity V is higher near the hot wall and corresponds to the maximum value (the maximum velocity is 19% higher than the peak value near the cold wall). It is interesting to note that in the near-wall region ($0.0 < X < 0.03$), the vertical velocity distributions for Boussinesq and non-Boussinesq solutions are nearly identical. Concerning the horizontal velocity U, the boundary layers near the upper and lower walls are not so thin as near the vertical wall and the peaks move separately to the nearest wall. The maximum peakoccursnear the upperwall (37% differences).

Effect of transport coefficients variation

In this section, computations are performed for Ra = 10^6 and for high temperature gradients (ε_b = 0.6). Some differences appear between solutions with constant and variable coefficients (μ^*, k^*). In fig. 7, the horizontal profiles of temperature show that the profiles are not symmetric even though the properties are constant. This indicates that this behavior is necessary due to a strong variation in density. In general, the temperature remains higher when the coefficients are variable especially at the core region.

The effect of properties variation on Nusselt number profiles is particularly observed near the horizontal walls (fig. 8), when the non Boussinesq solution for variable properties predicts greater values than the constant properties case.

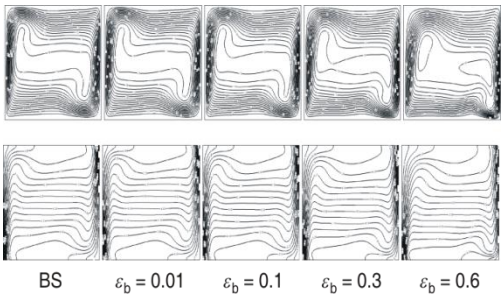

Figure 6. Streamlines (top) and temperature contours (bottom) at Ra = 10^6 for variable properties

If we compare the profiles of velocity components (figs. 9, 10), the effect of properties variation seems to be lower compared to the temperature. For the component V, the difference between the two profiles appears essentially for the peak values. Their locations as the boundary layers thickness are similar in both cases (a difference of 13% between peak values near the hot wall, and 2% for peaks near the cold wall). For the horizontal component U, the core region is influenced by the properties variations and the values are slightly greater

when the coefficients are constant. The impact of properties variation is more visible on the streamlines and the temperature contours as shown on fig. 11. The curves indicate a unicellular flow for constant (μ^*, k^*) while for variable properties, two secondary flows occur in the core of the cavity. This is accompanied by a significant shift between the curves of the isotherms.

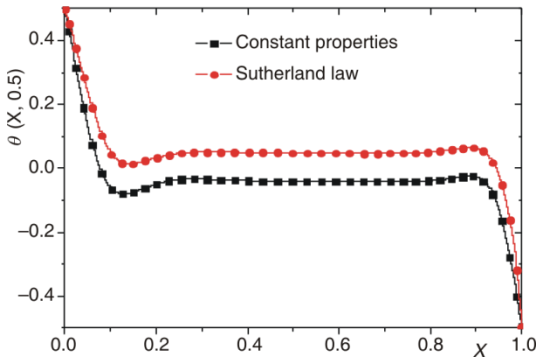

Figure 7. Cross-section of the temperature at mid-height cavity

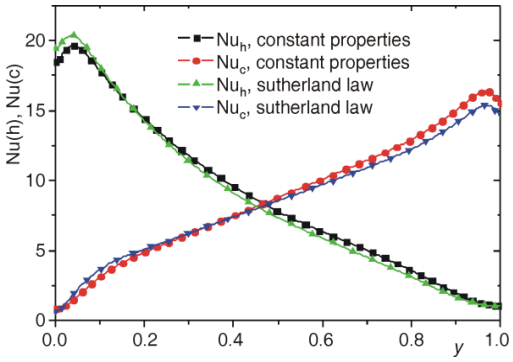

Figure 8. The distributions of local Nusselt numbers on the hot and cold walls for Ra = 10^6

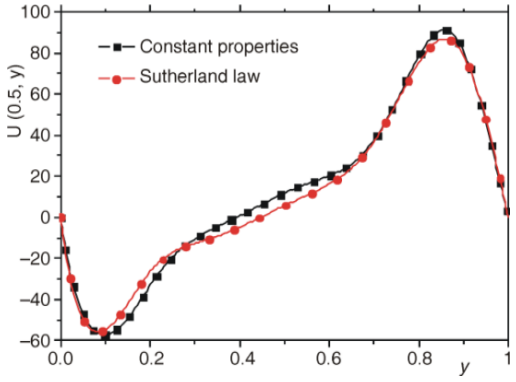

Figure 9. Horizontal velocity at the vertical cross-section at X = 0.5

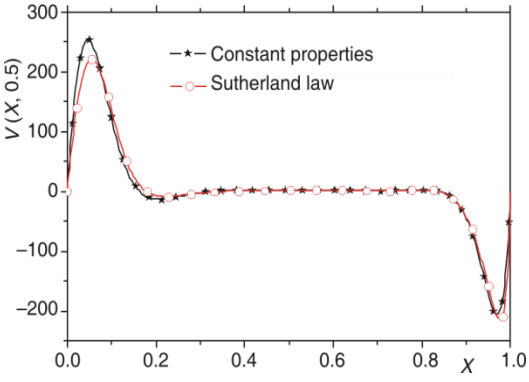

Figure 10. Vertical velocity at the horizontal cross-section at Y = 0.5

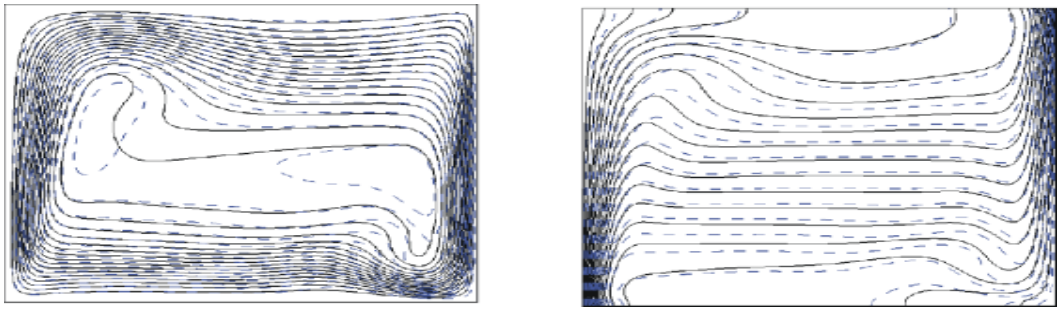

Figure 11. Streamlines (left) and temperature isolines (right) for constant properties (solid line) and Sutherland law (dashed line)

Conclusions

The aim of the present study is to investigate the effect of temperature gradient and properties transport variation on natural convection in the context of low Mach number formulation.

Results show that the Boussinesq approximation is not sufficient to simulate natural convective flow when the difference between the two vertical walls is high and the flow becomes more compressible.

The study shows that the symmetry of the flow is broken with increasing the Boussinesq parameter, and variation of thermophysical properties may have a significant influence on the heat transfer and on the fluid flow.

Nomenclature

c_p – specific heat, at constant pressure [$JKg^{-1}K^{-1}$]
c_v – specific heat at constant volume, [$JKg^{-1}K^{-1}$]
g – gravitational acceleration, [ms^{-2}]
H – height of the enclosure, [m]
k – thermal conductivity, [$Wm^{-1}K^{-1}$]
k^* – dimensionless thermal conductivity, [–]
Nu – convective Nusselt number, [–]
$\overline{P}$ – dimensionless thermodynamic pressure, [–]
Pr – Prandtl number, (= ν/α), [–]
p – total pressure, [= $p' + p_0 - \overline{p}$ (t)], [Pa]
p_0 – static pressure, [Pa]
p' – perturbed pressure, [Pa]
p_{dvn} – dynamic pressure, (= $p' + p_0$), [Pa]
$\overline{p}$ – mean thermodynamic pressure, [Pa]
Ra – Rayleigh number, [= $g\beta\Delta TH^3/(\nu\alpha)$], [–]
S – dimensionless surface, [–]
S_μ – Sutherland constant, [K]
T – dimensionless temperature, [K]
ΔT – temperature difference, (= $T_h - T_c$), [K]
t – time, [s]
U, V – dimensionless velocity-components, [–]
X, Y – dimensionless co-ordinates, [–]
x, y – Cartesian co-ordinates, [m]

Greek symbols

α – thermal diffusivity, (= $k/\rho Cp$), [m^2s^{-1}]
β – thermal expansion coefficient, [K^{-1}]
γ – specific heat ratio, (= c_p/c_v), [–]
ε_b – Boussinesq parameter, ($\Delta T/2T_0$), [–]
θ – dimensionless temperature, [= $(T - T_0)/\Delta T$], [–]
μ – dynamic viscosity, [$Kgm^{-1}s^{-1}$]
μ^* – dimensionless dynamic viscosity, [–]
ν – kinematic viscosity, [m^2s^{-1}]
ν^* – dimensionless kinematic viscosity, [–]
Ω – dimensionless control volume, [–]
Π – dimensionless pressure $= (p - \overline{p} + \rho_0 gy)/\rho_0(\alpha_0/H)^2$, [–]
ρ – fluid density, [kgm^{-3}]
ρ^* – dimensionless fluid density, [–]
τ – dimensionless time, [–]

Subscripts

avg – average value
BS – Boussinesq model
CP – Constant Properties
c – cold
LMN – low Mach number
max – maximum value
mid – midplane
min – minimum value
0 – reference state
h – hot

References

[1] Paolucci, S., On the Filtering of Sound from the Navier-Stokes Equations, Technical Report 82-8257, Sandia National Laboratories, 1982
[2] Suslov, S. A., Paolucci, S., Nonlinear Analysis of Convection Flow in a Tall Vertical Enclosure under Non-Boussinesq Conditions, *J. Fluid Mech.344* (1997), Aug., pp. 1-41
[3] Codina, R., A Stabilised Finite Element Method for Generalised Stationary Incompressible Flows, *Method Appl. Mech. Eng.*, *190* (2001), 20-21, pp. 2681-2706
[4] Vierendeels, J., *et. al*., A Multigrid Method for Natural Convective Heat Transfer with Large Temperature Differences, *Journal of Computational and Applied Mathematics*, *168* (2004), 1-2, pp. 509-517
[5] Bouafia, M., Daube, O., Natural Convection for Large Temperature Gradients around a Square Solid Body within a Rectangular Cavity, *Int. J. Heat and Mass Transfer*, *50* (2007), 17, pp. 3599-3615

[6] Chenoweth, D. R., Paolucci, S., Natural Convection in an Enclosed Vertical Air Layer with Large Horizontal Temperature Differences, *J. Fluid Mech.*, *169* (1986), Aug., pp. 173-210
[7] White, F. M., *Viscous Fluid Flow*, McGraw-Hill, New York, USA, 1974
[8] Patankar, S. V., *Numerical Heat Transfer and Fluid Flow*, McGraw-Hill, New York, USA, 1980
[9] Vierendeels, J., A Multigrid Semi-Implicit Line-Method for Viscous Incompressible and Low-Mach Number Flows on High Aspect Ratio Grids, *J. Comput. Phys*., *154* (1999), 2, pp. 310-341
[10] Heuveline, V., On Higher-Order Mixed FEM for Low Mach Number Flows: Application to a Natural Convection Benchmark Problem, *Int. J. Numer. Methods Fluids*, *41* (2003), 12, pp. 1339-1356
[11] Mizushima, J., Gotoh, K., Nonlinear Evolution of the Disturbance in a Natural Convection Induced in a Vertical Fluid Layer, *J. Phys. Soc. Japan*, *52* (1983), 4, pp. 1206-121

Paper submitted: August 10, 2013
Paper revised: June 18, 2014
Paper accepted: July 1, 2014